

# Seismic design method of high-performance structure based on gradient function

Ding-Hao Yu\*, Yuhuan Zhang, Cheng Zhou, Yaqiang Zhang and Gang Li

State Key Laboratory of Coastal and Offshore Engineering, Dalian University of Technology,  
Dalian 116024, China

(Received August 8, 2024, Revised October 17, 2024, Accepted November 3, 2024)

**Abstract.** As seismic research advances, the concept of seismic design that prioritizes both structural safety and post-earthquake operational functions has received increasing attention. Numerous high-performance structural systems with redundant members or damage-reduction elements have emerged continuously, and the structural function degrades progressively as different seismic defense lines are compromised. Therefore, this paper proposes a gradient functional seismic design method suitable for high-performance structures. By managing the damage sequence and degree of different seismic fortification lines in the structure, the structural function is reduced according to the expected gradient, ensuring structural resilience under different level of seismic fortification. This method categorizes the functional gradient into three stages: serviceability, damage control, and collapse prevention. By correlating structural function with component damage, the method translates the desired functional targets of the structure into specific damage targets for each component, establishing a seismic design process that considers diverse functional goals. The results of numerical example demonstrate the accuracy and practicability of this method.

**Keywords:** component damage; equivalent linearization method; gradient function; high-performance structure; seismic design

---

## 1. Introduction

Currently, domestic and foreign scholars mainly focus on the research and development of new systems or new components for high-performance structures, while the design theory lags relatively behind. Pollino *et al.* (2015) proposed a rocking steel frame combined with viscous dampers and mild steel yielding energy dissipation devices, which has self-centering ability. Dowden *et al.* (2015) proposed a self-centering steel plate shear wall, which reduces the structural damage by steel plate yielding energy dissipation and can eliminate the structural residual deformation. Zhu *et al.* (2020) designed a new type of grid-type friction damper with a dual energy dissipation mechanism, overcoming the disadvantage of a sharp reduction in post-yield stiffness of hysteretic dampers. Zhou *et al.* (2019) proposed the four-level seismic fortification objectives of the self-centering brace-rocking frame structural system and presented the displacement-based seismic design method of the structural system under the four-level seismic fortification objectives. Feng *et al.* (2018) studied the seismic design and performance of buckling-restrained braced

---

\*Corresponding author, Associate Professor, E-mail: ydh@dlut.edu.cn

frames with rocking walls (BRBF-RW) and proposed an elastic displacement spectrum-based seismic design method for BRBF-RW. Zhu *et al.* conducted a study on the seismic design of steel moment-resisting frames (MRFs) with self-centering viscous-hysteretic devices (SC-VHDs), and proposed the force-based design method (FBD) and direct displacement-based design method (DDBD).

However, due to the high redundancy of high-performance structures, components are gradually damaged, and the post-earthquake function gradually degrades, making it more difficult to restore the function. For various types of structural systems, the gradual failure of components ultimately results in a gradient decline in structural function. Therefore, it is urgent to establish a design theory that adapts to the gradient decline of high-performance structures to ensure that multiple defense lines play their roles in the expected order and meet the performance requirements of different seismic levels.

The seismic code adopts the design concept of "no damage under minor earthquakes, repairable under moderate earthquakes, and no collapse under major earthquakes". The elastic design ensures the performance requirements under minor earthquakes, but it is difficult to clarify the damage evolution sequence of each component after the structure enters the damaged state. The performance-based seismic design SEAOC Vision (2000) determines the performance target according to the use of the building and the seismic level, so that the structure has the expected performance level in future earthquakes. Currently, some studies (Clayton *et al.* 2011, Han 2008, Ding 2004), have given the design methods of functional targets under different seismic fortification levels in self-centering steel frame structures and self-centering braced-rocking frame structures. Besides, structural reliability analysis under different fortification levels has also been extensively studied. However, most methods are based on the characteristics of specific systems and have limited applicability, without fully considering the common characteristics of the gradient decline of structural function. Starting from the perspective of gradient function will help to establish a widely applicable seismic design theory for high-performance structures.

Therefore, this paper proposes a gradient functional seismic design method for high-performance structures and verifies its effectiveness through examples.

## 2. The gradient functional seismic design method

### 2.1 Characteristics of the gradient function of high-performance structures

High-performance structures have multiple seismic defense lines, and the gradual destruction of different components under the action of earthquakes causes the structural function to gradually decrease, presenting the characteristics of a gradient function.

### 2.2 Design process

The damage and destruction of components are directly related to the reduction of structural function. Firstly, the relationship between structural function loss and component damage is established. Based on this, the gradient functional targets under different seismic levels are transformed into the expected damage targets of each component. Further, through the design of bearing capacity and deformation capacity, the damage of each component in the structure meets the design requirements under different seismic levels.

### 3. Quantitative relationship between structural function and component damage

#### 3.1 Component damage model

A calculation model describing the degree of component damage is established, and on this basis, the gradient functional target of the structure is quantified. In this paper, the stiffness ratio damage model proposed by Du *et al.* (1991) is adopted, and the ratio of the secant stiffness at the maximum displacement of the component to its initial stiffness is used as the quantitative basis for the degree of damage, as shown in Eq. (1)

$$D = 1 - k_{eq}/k_0 \quad (1)$$

Where  $D$  represents the component damage index,  $k_{eq}$  is the secant stiffness of the component, and  $k_0$  is the initial stiffness of the component.  $D$  varies within the interval  $[0, 1]$ , where 0 and 1 respectively indicate that the component is in the initial elastic state and has completely lost its bearing capacity.

#### 3.2 Relationship between structural function and component damage

In this paper, according to the functional attributes and importance of components, the components of high-performance structures are divided into four categories: expected non-damaged components (such as columns, walls and other key load-bearing components), important components, general components, and secondary components. By grouping, the damage sequence under an earthquake is clarified. It is assumed that the secondary components are damaged first, and as the earthquake intensity increases, it gradually affects the general components, important components, until the expected non-damaged components are damaged, resulting in the collapse of the structure.

The high-performance structure contains  $W$  different levels of component groups ( $D_i$ ,  $1 \leq i \leq W$ ). The damage state of the first component groups can describe the relationship between the overall structural function and the damage of each component group as shown as

$$Q_F = \begin{cases} 1, & m < 1 \\ 1 - \sum_{i=1}^m \beta_i Q_{D_i}, & 1 \leq m \leq W \end{cases} \quad (2)$$

where  $Q_F$  is the structural function index,  $Q_{D_i}$  is the damage degree of the component group  $D_i$ , and  $\beta_i$  is the functional weight coefficient of the component group  $D_i$ . The functional weight coefficient increases with the level of the component group.

The principles for allocating the damage index of each component group selected in this paper are as follows:

- When multiple component groups are simultaneously in the expected damage state, a higher expected damage index is set for the lower-level component group, and a lower expected damage index is set for the higher-level component group.
- The average damage degree within the component group is taken as the target judgment standard.
- As the structural function target gradually decreases, the damage index of each component group increases step by step.

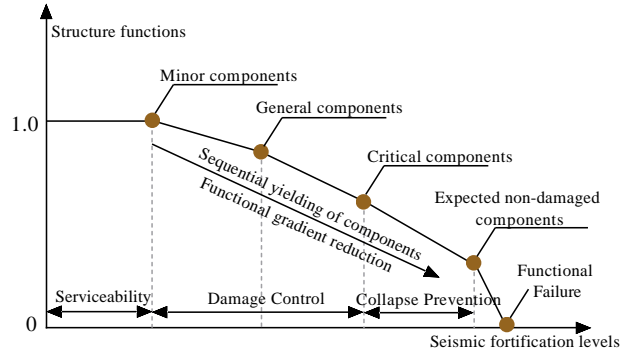


Fig. 2 Test specimen dimensions

Table 1 Range of structural function index in different functional stages

Functions	Serviceability	Damage Control	Collapse Prevention
Index	1	0.6~1	0.3~0.6

As shown in Figure 1, when the seismic fortification level is small, each component group has not entered the damaged state, and the structure is in the serviceability functional stage; as the seismic fortification level gradually increases, the structure transitions from the serviceability functional stage to the damage control functional stage; when the damage degree of the important component group is large, the structure forms a significant overall yielding mechanism, the structural damage degree is heavy, but the expected non-damage component group has not yet entered the damaged state, and the structure transitions from the damage control to the collapse prevention stage; as the seismic fortification level continues to increase, the expected non-damage component group is damaged and destroyed, and the structure enters the collapse stage.

#### 4. The gradient functional design method for structures

Defining the functional target under different seismic fortification levels is an important step in the gradient functional design. In this method, the functional target in the serviceability stage is set as  $Q_1$ ; multiple functional targets are set in the damage control stage, namely from  $Q_2$  to  $Q_{N-1}$ ; the functional target in the collapse prevention stage is set as  $Q_N$ , where  $N$  is the number of functional gradients. This section uses different methods to design each functional stage.

##### 4.1 Serviceability functional stage

In the serviceability stage, each component group is elastic, and the functional target index  $Q_1$  is 1. After determining the seismic fortification level, the internal force requirements of each component under vertical and lateral loads can be calculated. To make sure the structure is safe, the combination of earthquake and gravity is used to determine the bearing capacity during this stage, can be computed as

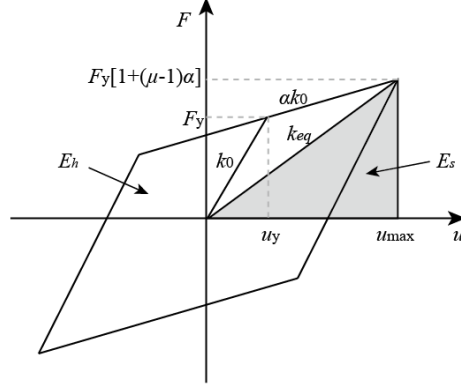


Fig. 2 Secant stiffness and hysteretic energy dissipation of bilinear elastoplastic model

$$S_D = \gamma_G S_G + \gamma_E S_{EK} \quad (3)$$

where  $S_D$  is the bearing capacity in the serviceability stage;  $S_G$  is the gravity;  $S_{EK}$  is the earthquake action effect;  $\gamma_G$  and  $\gamma_E$  are the partial coefficients of gravity and earthquake respectively.

#### 4.2 The damage control function stage

The functional design target  $Q_m$  ( $2 \leq m \leq N-1$ ) is transformed into the damage index of each component group. The structure's damage distribution patterns vary depending on its functional targets. A calculation method that considers these patterns needs to be established.

This paper considers the damaged components in the process of structural functional gradient change by using the equivalent linearization method with a lower stiffness  $k_{eq}$  and a higher damping ratio  $\zeta_{eq}$ . This paper uses the equivalent linearization model based on secant stiffness to determine the equivalent stiffness and damping ratio of damaged components. The equivalent stiffness is the secant stiffness at maximum displacement  $u_{max}$ , and the equivalent damping ratio  $\zeta_{eq}$  is the sum of the additional damping ratio  $\zeta_a$  and the initial damping ratio  $\zeta_0$ , as shown in Eq. (4(b)).

$$\zeta_a = \frac{1}{4\pi} \frac{E_h}{E_s} \quad (4a)$$

$$\zeta_{eq} = \zeta_0 + \zeta_a \quad (4b)$$

In the equation,  $E_h$  is the hysteretic energy dissipation of the expected damaged component in a single symmetric loading cycle, and  $E_s$  is the elastic strain energy of the component.

The force characteristics of the expected damaged components conform to the bilinear elastoplastic model shown in Fig. 2. The formulas for the equivalent stiffness  $k_{eq}$  and the equivalent damping ratio  $\zeta_{eq}$  are shown in the following equations.

$$k_{eq} = k_0 \left[ \frac{1}{\mu} + \alpha \left( 1 - \frac{1}{\mu} \right) \right] \quad (5)$$

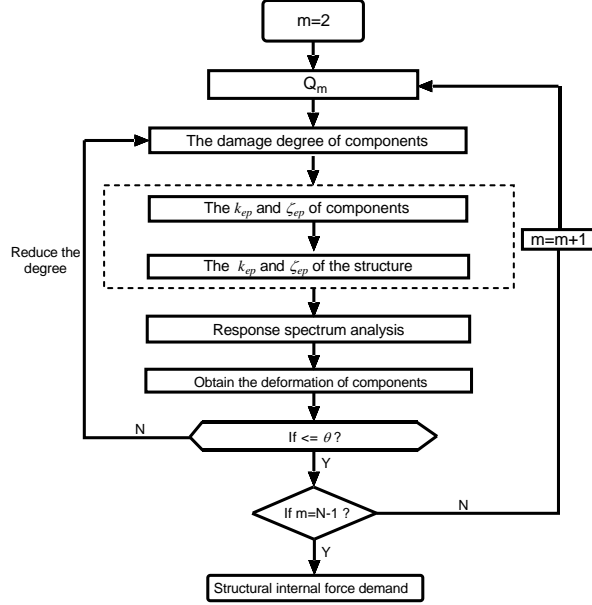


Fig. 3 Flow chart of structural design in damage control function stage

$$\zeta_{eq} = \frac{2(\mu-1)(1-\alpha)}{\pi\mu(1+\alpha\mu-\alpha)} + \zeta_0 \quad (6)$$

In the equations,  $k_0$  is the initial stiffness,  $\mu$  is the ductility coefficient, and  $\alpha$  is the post-yield stiffness coefficient. Substituting Eq. (5) into Eq. (1) shows the target ductility coefficient  $\mu$  and the damage index  $D$  of the expected damaged component can be established as

$$\mu = \frac{1-\alpha}{1-\alpha-D} \quad D > 0 \quad (7)$$

Fig. 3 shows the design process of this method in the damage control function stage, and the steps are as follows:

- Determine the functional target  $Q_m$  and the damage degree of the components, and determine the target ductility based on Eq. (7). For the initial calculation, let  $m = 2$ .
- Determine the equivalent stiffness and damping ratio respectively.
- Create a linear structure. Calculate the equivalent modal damping ratio of the equivalent linear structure using the energy-weighted average composite damping ratio method. See Eq. (8).

$$\zeta_{eq,i} = \frac{\sum_n E_{s,i,n} \zeta_{a,i,n}}{\sum_n E_{s,i,n}} + \zeta_0 \quad (8)$$

In the equation,  $\zeta_{eq,i}$  is the equivalent modal damping ratio of the  $i$ -th mode,  $\zeta_{a,i,n}$  is the equivalent damping ratio of the  $n$ -th component, and  $E_{s,i,n}$  is the elastic strain energy of the  $n$ -th component when the equivalent linear structure deforms according to the  $i$ -th mode.

1) Use the mode-superposition response spectrum method to calculate the seismic corresponding to the  $Q_m$ , and obtain the internal force demand and inter-story displacement angle distribution of the components.

2) If the inter-story drift angle limit must be met, verification should be performed based on the results from Step 4. If it does not meet the requirements, adjust the damage target and redesign. For multiple gradient functional targets, it is unnecessary to set limits for each expected functional target. In addition, performance indicators can be added according to the characteristics of the structure.

3) Use Eq. (9) to calculate the bearing capacity demand of the expected damaged components of the structure.

$$S_{K,m} = S_G + S_{EK} \quad (9)$$

In the equation,  $S_{K,m}$  is the bearing capacity;  $S_G$  and  $S_{EK}$  have been explained previously.

4) When the current functional target is  $Q_{N-1}$ , proceed to the next step; otherwise, change the functional target and recalculate.

5) Take the maximum value of the bearing capacity demand in the serviceability and damage control function stages as its design bearing capacity, as shown in Eq. (10).

$$S_{K,max} = \max\{S_{K,2}, \dots, S_{K,m}, \dots, S_{K,N-1}, S_D\} \quad (10)$$

In the equation,  $S_{K,max}$  is the design bearing capacity of a damaged component group  $D_i$ , and  $S_{K,m}$  is the bearing capacity in the damage control function stage.

### 4.3 The collapse prevention function stage

The collapse prevention function stage is designed to prevent collapse in rare earthquake. This method conducts two aspects in this stage: 1) The bearing capacity design of the expected non-damaged component group; 2) The deformation capacity design of the expected damaged components. Fig. 4 shows the design process of the collapse prevention function stage, and the steps are as follows:

1) Determine the  $Q_N$ . The process is described in reference. Add a coefficient  $\gamma$  to correct the bearing capacity of the expected non-damaged component group. Then determine the bearing capacity demand in the collapse prevention function stage according to Eq. (11).

$$S_C = (S_G + S_{EK}) \times \gamma \quad (11)$$

In the equation,  $S_C$  is the bearing capacity of the expected non-damaged component group in the collapse prevention function stage.

2) Verify if the overall function index maximum inter-story displacement angle meet the limit requirements. If not, increase the bearing capacity and recalculate.

3) The design bearing capacity is the highest among the stage of serviceability, damage control, and collapse, as shown in Eq. (12).

$$S_W = \max\{S_D, S_K, S_C\} \quad (12)$$

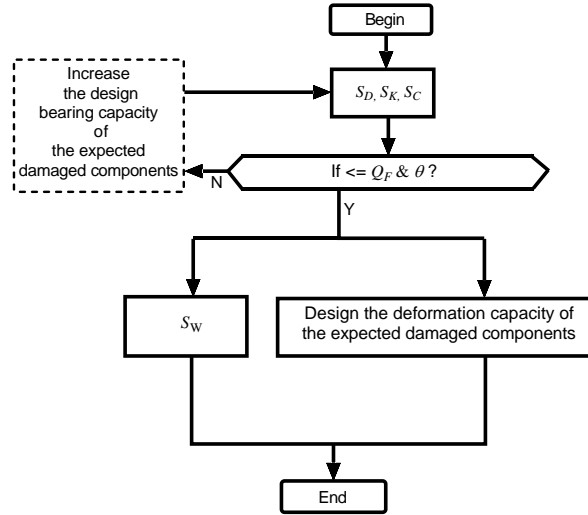


Fig. 4 Design flow chart of collapse prevention function stage

In the equation,  $S_w$  is the design bearing capacity of the expected non-damaged component group, and  $S_K$  is the bearing capacity demand in the damage control stage.

4) Based on the ductility of damaged components in step 1) and the relationship between the ultimate displacement angle and stirrup in beam-column components <sup>[18-19]</sup>, design the deformation capacity of the expected damaged components.

## 5. Design process

Fig. 5 shows the seismic design process of high-performance structures based on gradient function. Firstly, determine the expected damage targets of components under different seismic fortification levels, and clarify the damage order and degree of components. Then, calculate the design parameters under different functional targets based on the equivalent linearization theory. For the expected damaged components, the bearing capacity design should meet the maximum internal force demand in the serviceability and damage control stages, and the ductility demand in the collapse prevention stage is used as the basis for the deformation capacity design. For the expected non-damaged components, only the bearing capacity design is carried out, and it is necessary to ensure that they remain undamaged in each stage. The design basis is the maximum internal force demand in the three stages.

## 6. Example design

### 6.1 Project overview

To verify the feasibility of the design method in this paper, a new type of high-performance frame gradient shear wall structure is proposed to be designed. Low-strength concrete parts,

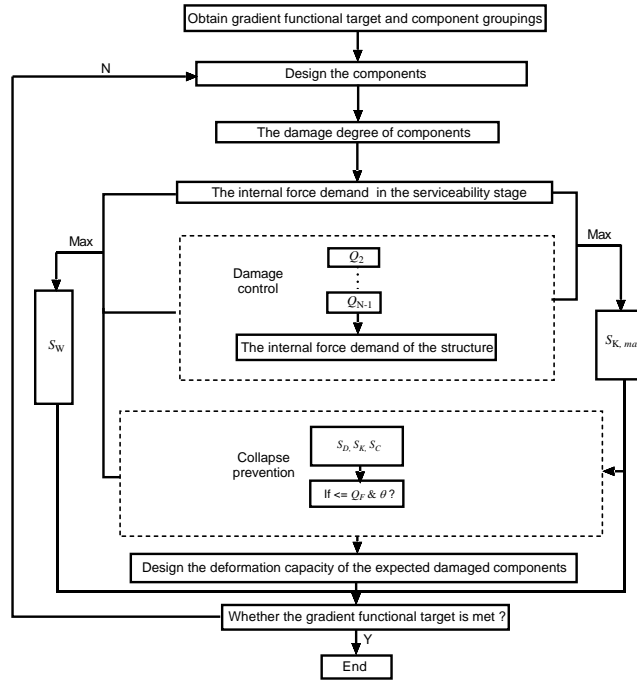


Fig. 5 The flow chart of seismic design of high-performance structures based on gradient function

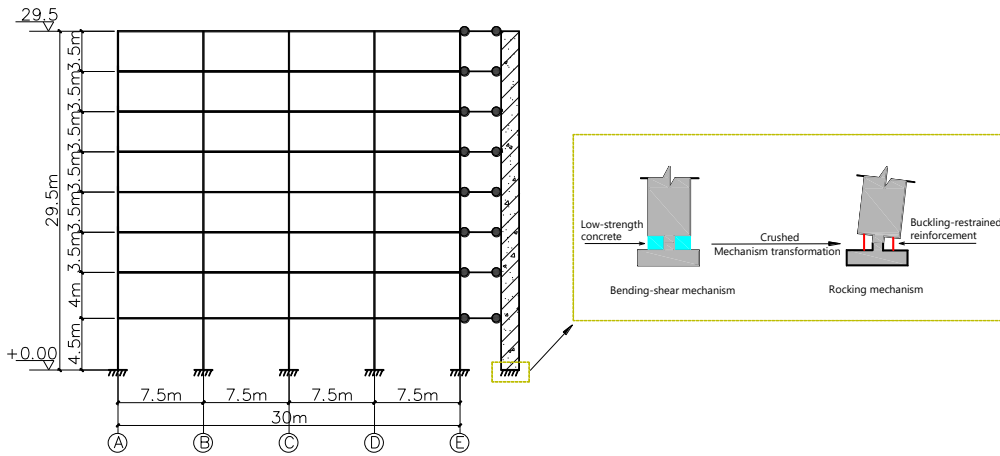


Fig. 6 Frame gradient shear wall structure

buckling-restrained reinforcement groups and rocking supports are set at the bottom of the structure wall. The construction measures are detailed in reference [20], and the schematic diagram of the model is shown in Figure 6. The gradient shear wall is hinged to the frame by connecting rods. The specific design parameters of the model are detailed in Appendix A.

Table 2 Grouping of frame gradient shear wall structure members <sup>[5]</sup>

	Expected Non - damaged Components	Important Components	General Components	Minor Components
Structural Components	frame columns, gradient shear walls	frame beams, bottom column feet	buckling - restrained reinforcement	low - strength concrete parts
Functional Weight Coefficient $\beta_i$	0.35	0.3	0.25	0.1

Table 3 Gradient functional design objectives of frame gradient shear wall structures

Functions	Serviceability	Damage Control		Collapse Prevention
Seismic fortifications	Minor	Medium-minor	Moderate	Major
PGA/g	0.07	0.14	0.2	0.4
Index	1	0.9	0.8	0.55
$\theta$	1/800	—	1/300	1/100
DCF	—	—	—	1.5

## 6.2 Design process

### 1) Gradient Functional Design Objectives and Component Grouping

The component grouping situation and the corresponding functional weight coefficients are detailed in Table 2. To prevent the formation of any weak layers, even when the gradient shear wall enters the rocking stage, the wall must remain undamaged. Therefore, both the wall and the frame columns are classified as part of the expected non-damaged component group.

To accurately guide the gradient change of the structural function, based on the three-level seismic fortification standard, a medium - minor earthquake design level is added between the minor earthquake and the moderate earthquake. Table 3 gives the gradient functional design objectives of the structure and the inter-story displacement angle limits under different earthquake intensities. Since the rocking wall can uniformize the inter-story displacement and avoid the appearance of weak layers, the inter-story displacement non-uniformity coefficient DCF proposed by Macrae *et al.* (2004) is simultaneously used as a supplementary design performance index for major earthquakes. The definition of DCF is expressed as

$$DCF = \theta_{\max}/(u_r/H) \quad (13)$$

In the equation,  $\theta_{\max}$  is the maximum inter-story displacement angle of the structure,  $u_r$  is the displacement of the structure vertex, and  $H$  is the total height of the structure. Table 3 gives the DCF target value for the example of a major earthquake.

### 2) Preliminary Design of Structural Components

The preliminary design results of the frame components are shown in Table 4. In the serviceability stage, the gradient shear wall can be regarded as a conventional shear wall, and the stiffness characteristic value  $\lambda$  of the wall-frame structure is used for preliminary design. Huang *et al.* studied that the optimal stiffness characteristic value interval of the hinged wall-frame structure is approximately  $\lambda=1\sim 2.5$ , and here  $\lambda=2.5$  is taken. According to the preliminary design results, the cross-sectional moment of inertia demand of the gradient shear wall in the serviceability stage is determined to be  $I_{w,1}=2.53 \text{ m}^4$ .

Table 4 The preliminary design result of frame

Floors	Heights(mm)	Column Sections(mm)	Beam Sections(mm)
1	4500	600×800	350×750
2	4000	600×800	350×750
3-4	3500	600×800	350×750
5-7	3500	600×600	300×750
8	3500	600×600	300×750

Table 5 Damage targets of each structural component group

Seismic Fortifications	Expected non-damaged Components	Important Components	General Components	Minor Components
Minor	0	0	0	0
Medium-minor	0	0	0	1
Moderate	0	0	0.4	1
Major	0	0.5	0.8	1

After the low-strength concrete parts are crushed and withdrawn from work, the structure is transformed into a frame - rocking wall structure. Macrae *et al.* (2004) studied that the DCF of this structure depends on the stiffness coefficient  $\alpha$ , and its definition is as shown in Eq. (14).

$$\alpha = EI/k/h^3 \quad (14)$$

In the equation,  $EI$  is the flexural stiffness of the rocking wall section,  $k$  is the lateral stiffness of the main frame layer, and  $h$  is the floor height; Qu (2010) took the DCF of the frame structure as the control target and established the relationship between the structure stiffness coefficient  $\alpha$  and the number of layers  $N$ , as shown in the following equation.

$$\alpha = 0.148N - 0.368 \quad (15)$$

This paper takes the DCF value corresponding to the elastic first-order mode shape of the main frame as the target value, and combines the preliminary design results in Table 4 to determine the DCF value of the structure under a major earthquake to be 1.5. According to Eq. (15) the stiffness coefficient is calculated to be  $\alpha=0.82$ , and substituting it into Eq. (14) calculates the cross-sectional moment of inertia demand of the gradient shear wall in the rocking state to be  $I_{w,2}=0.7 \text{ m}^4$ . Taking the larger value of the cross-sectional moment of inertia demand of the gradient shear wall in the two states as the design basis, the preliminary selection of the gradient shear wall section size is  $0.36 \text{ m} \times 4.5 \text{ m}$ .

### 3) Component Damage Target Setting

According to Table 3 and Eq. (2), determine the expected damage targets of each structural component group under different seismic fortification levels, as shown in Table 5. It should be noted that the low-strength concrete parts are not ductile components and once crushed, they withdraw from work, so the damage index has only 0 (undamaged) and 1 (damaged).

Table 6 Expected ductility coefficient of each structural component group

Seismic Fortifications	Expected non-damaged Components	Important Components	General Components
Minor	-	-	-
Medium-minor	-	-	-
Moderate	-	-	1.67
Major	-	2	5

Note: The symbol “-” indicates that the component is in an elastic state

Table 7 Design parameters and design results of structural damage components

Expected Damaged Components	Tensile Zone of Frame Beams		Unilateral Buckling-restrained Reinforcement	Each Side of Bottom Column Feet	Low-strength Concrete Parts	
	Floors 1~4	Floors 5~8				
Design parameters	Moments 593 kN·m	Moments 530 kN·m	Flexural stiffness 2.1E9 N·m <sup>2</sup>	Flexural yield strength 5584 kN·m	Moments 600 kN·m	Compressive strength 8.24 N/mm <sup>2</sup>
Results	Area 2945 mm <sup>2</sup>	Area 2281 mm <sup>2</sup>	Area 3142 mm <sup>2</sup>	Length 1.5 m	Area 1005 mm <sup>2</sup>	Concrete C20

Taking the post-yield stiffness coefficient  $\alpha=0$ , calculate the target ductility coefficients of the component groups under different seismic fortification levels according to Eq. (7), as shown in Table 6. The low-strength concrete parts are non-ductile components, and only the coefficients of the expected non-damaged, important and general component groups are given in the table.

#### 4) Design of the Serviceability and Damage Control Function Stages

According to the target ductility coefficients in Table 6, the internal force demands of the expected damaged components in the serviceability stage under minor earthquake and in the damage control stages under medium-minor earthquake and moderate earthquake can be calculated respectively by using the aforementioned methods. Further, the design bearing capacity of the expected damaged components is determined according to Eq. (10). Table 7 shows the design parameters and design results of each expected damaged component of the structure. In addition, Fig. 7 shows the inter-floor displacement angle distribution of the structure under moderate earthquake, and it shows that the structure meets the limit requirements of the inter-floor displacement angle.

#### 5) Design of the Structure in the Collapse Prevention Function Stage

Fig. 8 shows the inter-story displacement angle of the structure and the ductility requirements of the frame beam ends. The maximum inter-story displacement angle of the structure is 1/148, which is less than the limit value of 1/100. According to Eq. (2), the overall function index of the structure is calculated to be 0.58, and both meet the expected requirements. Further, according to the inter-story displacement angle of the structure, the DCF value can be calculated to be 1.23 according to Eq. (13), which is less than the design value of 1.50. The smaller the DCF, the smaller the dispersion degree of the inter-story deformation of the structure, and the more uniform the inter-story deformation. The additional damping ratios of components in each stage and the equivalent damping ratio of the whole structure of the example structure are given in Appendix B.

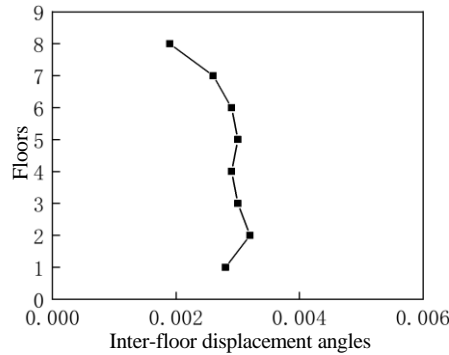


Fig. 7 Inter-floor displacement angle of structure under moderate earthquake

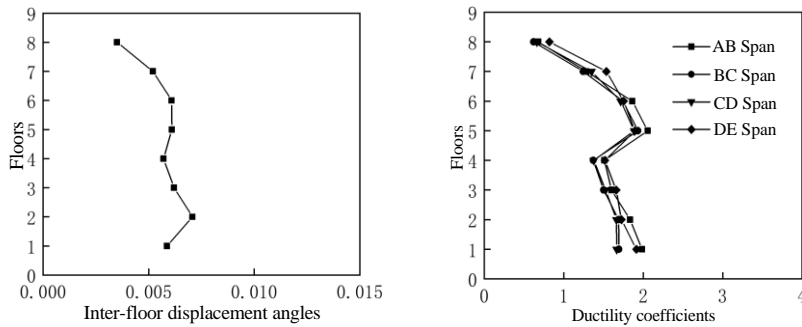


Fig. 8 Inter-story displacement angle and beam ends ductility requirements under major earthquake

Table 8 Requirements for deformation capacity of frame beam ends and design of stirrup

Floors	Section Size (mm)	Ductility $\mu_{dem}$	Stirrup Characteristic Values $\lambda_{v,dem}$	Actual Stirrup
1~4	350×750	1.9	0.071	φ8@100(4)
5~8	300×750	2.1	0.073	φ8@100(4)

Using the design methods of reinforced concrete beams and columns proposed by Qian *et al.* (2007), combined with the stirrup construction requirements in the specification, the stirrup design of the frame beam ends and the bottom column feet is carried out, and the design results are shown in Table 8. According to Eq. (12), the design bearing capacities of the frame columns and the gradient shear wall walls are determined respectively and the reinforcement design is carried out, and the design results are shown in Table 9.

### 6.3 Seismic performance analysis

To verify the effectiveness of the design method proposed in this paper, four ground motions are selected from the PEER/NGA database in the United States for seismic performance analysis.

Table 9 Design results of expected non-damaged components

Expected non-damaged Components	Reinforcement on Each Side of Frame Columns (mm <sup>2</sup> )		Reinforcement on Each Side of Frame Columns	
	Floors 1~4	Floors 5~8	End Longitudinal Reinforcement (mm <sup>2</sup> )	Horizontal and Vertical Distributed Reinforcement
Results	3079	2454	4926	φ12@150

Table 10 Basic information of selected ground motion records

Numbers	Names	Years	Stations	Magnitudes	PGA/g
RSN-1	Hector Mine	1999	Hector	7.1	0.26
RSN-2	Imperial Valley	1979	El Centro Array #11	6.5	0.36
RSN-3	Kocaeli Turkey	1999	Arcelik	7.5	0.21
RSN-4	Northridge	1994	Canyon Country-WLC	6.7	0.40

Table 11 Model information in ABAQUS

Categories	Projects	Properties
Element	Beams	B21
	Columns	B21
	Shear Walls	S4
Materials	Concrete	$f_c = 200$ MPa
	Rebars	$f_y = 235$ MPa
Mesh Density	Beams & Columns	30 mm
	Shear Walls	50 mm
	Rebars	20 mm

Note:  $f_c$  is the compressive strength of C20 concrete,  $f_y$  is the yield stress of the rebars

The detailed earthquake information is shown in Table 10. The ABAQUS software is used for numerical simulation, and the information of model is listed in Table 11.

Fig. 9 shows the distribution of plastic hinges of the structure under different intensities of RSN-1 earthquake. There are no plastic hinges under minor earthquake (Fig. 9(a)), and the whole structure is in an elastic working state; under medium-minor earthquake, the damage is concentrated on the low-strength concrete parts, and the low-strength concrete parts have been crushed, and the buckling-restrained reinforcement groups have not yielded; under moderate earthquake, plastic hinges are formed at the bottom of the gradient shear wall (Fig. 9(b)), the buckling-restrained reinforcement groups have yielded, and some column feet of the main frame have formed plastic hinges; under major earthquake, the main frame basically forms the expected beam hinge mechanism (Fig. 9(c)), and it is in the collapse prevention function stage, and no significant weak layer appears.

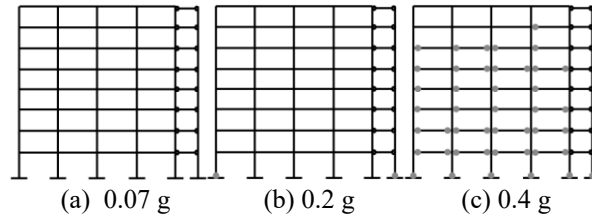


Fig. 9 Distribution of structural plastic hinges

Table 12 Average damage index of each structural components

Seismic Fortifications	Expected non-damaged Components	Important Components	General Components	Minor Components
Minor	0	0	0	0
Medium-minor	0	0	0	1
Moderate	0	0	0.43	1
Major	0	0.23	0.77	1

Table 13 The function index of the structure under different intensity RSN-1 seismic excitation

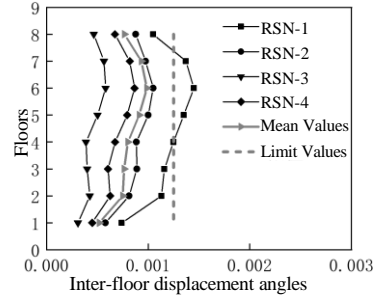
Seismic Fortification	Minor	Medium-minor	Moderate	Major
Function Index	1	0.9	0.79	0.63

The average damage index of each structural component group under different intensities of RSN-1 earthquake is shown in Table 12. Table 13 shows the function index of the structure under different intensities of RSN-1 earthquake, and both reach the expected design target requirements. In summary, each component of the structure can enter the damage in an expected order, and the function index meets the expected requirements.

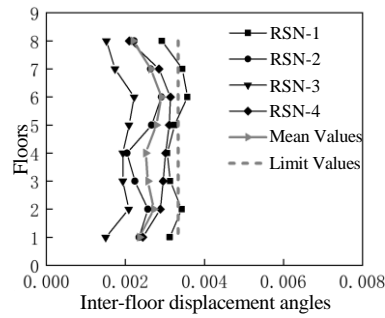
The inter-story displacement angle of the structure under different intensities of earthquake is shown in Fig. 10, and the average inter-story displacement angle under each earthquake action meets the corresponding limit requirements. In addition, the DCF value of the structure under major earthquake is 1.26, which is less than the design value of 1.50. This shows that the structure effectively controls the non-uniformity of inter-story displacement during the collapse prevention stage, achieving the design goal of preventing weak layer failure.

## 7. Conclusions

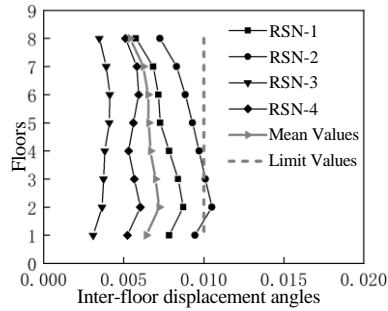
This paper proposes a seismic design method for high-performance structures based on gradient function. The structural function is divided into three gradient stages: serviceability, damage control, and collapse prevention. By establishing the relationship between structural function loss and component damage, the gradient functional targets are transformed into the expected damage targets of components. The design methods for the bearing capacity and deformation capacity of



(a) 0.07 g



(b) 0.2 g



(c) 0.4 g

Fig. 10 Inter-story displacement angle of the structure during earthquakes of different intensities

components under different stages are given. Through reasonable design, the components can be progressively damaged as expected under different seismic levels, achieving the gradient change of structural functions, providing a new idea for the seismic design of high-performance structures. Meanwhile, the results of the example verify the applicability and accuracy of this method.

The methods of this study provide a significant insight into the structural earthquake-resistant design. It can be concluded that the progressive damage framework enhances design safety, helping to maintain structural stability and protect occupant safety under severe seismic conditions. It should be noted that this method is specifically developed for frame-shear wall structures, and its applicability to other types of structures (such as large-span or non-frame structures) has not yet been extended. Future research will further verify and expand the method's applicability to enhance its practical utility.

## References

- Clayton, P.M., Dowden, D.M. and Purba, R. (2011), "Seismic design and analysis of self-centering steel plate shear walls", *Proceedings of the structures Congress 2011*. Reston, VA: American Society of Civil Engineers, 748-757. [https://doi.org/10.1061/41171\(401\)66](https://doi.org/10.1061/41171(401)66).
- Ding, J. (2004), "Theory and method of direct damage-based seismic capacity design of reinforced concrete frame structures", M.D. Dissertation, Xi'an University of Architectural and Technology, XiAn.
- Dowden, D.M., Clayton, P.M., Berman, J.W., Bruneau, M., Lowes, L.N. and Tsai, K.C. (2015), "Full-scale pseudodynamic testing of self-centering steel plate shear walls", *J. Struct. Eng.*, **142**(1), 04015100. [https://doi.org/10.1061/\(ASCE\)ST.1943-541X.0001367](https://doi.org/10.1061/(ASCE)ST.1943-541X.0001367).
- Du, X. and Ou, J.P. (1991), "Seismic damage assessment model for building structures", *World Earthq. Eng.*, (3), 52-58.
- Feng, Y., Zhang, Z., Chong, X., Wu, J. and Meng, S. (2018), "Elastic displacement spectrum-based design of damage-controlling BRBFs with rocking walls", *J. Constr. Steel Res.*, **148**, 691-706. <https://doi.org/10.1016/j.jcsr.2018.06.022>,
- Fu X., Du, W.L., Li, G., Dong, Z.Q. and Li, H.N. (2024), "A data-driven method for the reliability analysis of a transmission line under wind loads", *Steel Compos. Struct.*, **52**(4), 461-473. <https://doi.org/10.12989/scs.2024.52.3.461>.
- Fu, Z., Tian, L., Luo, X., Pan, H. and Liu, J. (2024), "Study on the influence of structural and ground motion uncertainties on the failure mechanism of transmission towers", *Earthq. Struct.*, **26**(4), 311-326. <https://doi.org/10.12989/eas.2024.26.4.311>.
- GB 50011-2010 (2010), *Code for Seismic Design of Buildings*, China Architecture & Building Press, Beijing.
- Han J.P., Yan, R. and Li, H. (2008), "Performance -based seismic design for structures with viscoelastic dampers", *J. Earthq. Eng. Eng. Vib.*, (1), 175-181. <https://doi.org/10.13197/j.eeev.2008.01.026>.
- Jacobsen, L.S. (1930), "Steady forced vibrations as influenced by damping", *J. Fluids Eng.*, **20**(3), 196-223. <https://doi.org/10.1785/BSSA0200030196>.
- Jouneghani, H.G., Haghollahi, A. and Beheshti-Aval, S. (2020), "Experimental study of failure mechanisms in elliptic-braced steel frame", *Steel Compos. Struct.*, **37**(2), 175-191. <https://doi.org/10.12989/scs.2020.37.2.175>
- Li, G. and Li, R.H. (2022), "An innovative shear wall with gradient phases and experimental study on the seismic behavior", *J. Build. Struct.*, **43**(3), 46-56. <https://doi.org/10.14006/j.jzjgxb.2020.0319>.
- Liu, Q. and Wang, M. (2020), "Seismic reliability analysis of structures based on cumulative damage failure mechanism", *Earthq. Struct.*, **18**(4), 519-526. <https://doi.org/10.12989/eas.2020.18.4.519>.
- Macrae, G.A., Kimura, Y. and Roeder, C. (2004), "Effect of column stiffness on braced frame seismic behavior", *J. Struct. Eng.*, **130**(3), 381-391. [https://doi.org/10.1061/\(ASCE\)0733-9445\(2004\)130:3\(381\)](https://doi.org/10.1061/(ASCE)0733-9445(2004)130:3(381)).
- Pollino, M. (2015), "Seismic design for enhanced building performance using rocking steel braced frames", *Eng. Struct.*, **83**, 129-139. <https://doi.org/10.1016/j.engstruct.2014.11.005>.
- Qian, J.R. and Xu, F.J. (2007), "Displacement-based deformation capacity design of RC columns", *Build. Struct.*, (12), 30-32. <https://doi.org/10.19701/j.jzjg.2007.12.009>.
- Qian, J.R. and Xu, F.J. (2007), "Displacement-based deformation capacity design method of reinforced concrete beams", *Sichuan Building Sci*, (2), 1-3.
- Qu, Z. (2010), "Study on seismic damage mechanism control and design of rocking wall-frame structures", Ph.D. Dissertation, Tsinghua University, BeiJing.
- Qu, Z. and Ye, L.P. (2011), "Seismic design methodology based on damage mechanism control for reinforced concrete structures", *J. Build. Struct.*, **32**(10), 21-29. <https://doi.org/10.14006/j.jzjgxb.2011.10.003>.
- Rosenblueth, E. and Herrera, I. (1964), "On a kind of hysteretic damping", *J. Eng. Mech. - ASCE*, **90**(4), 37-48. <https://doi.org/10.1061/JMCEA3.0000510>.
- SEAOC Vision 2000 (1995), A framework for performance-based engineering, structural engineering association of California.

- Yang, Y. (2012), "Optimal design for lateral stiffness of frame-shear wall structure", M.D. Dissertation, Hefei University of Technology, Hefei.
- Ying, Z. and Anqi, G. (2019), "Displacement-based seismic design of self-centering shear walls under four-level seismic fortifications", *J. Build. Struct.*, **40**(3), 118-126. <https://doi.org/10.14006/j.jzjgxb.2019.03.012>.
- Zhu, L.H., Li, G. and Dong, Z.Q. (2020), "An experimental study and numerical simulation of lattice-shaped friction devices", *J. Vib. Shock*, **39**(4), 96-105. <https://doi.org/10.13465/j.cnki.jvs.2020.04.012>.
- Zhu, L.H., Li, G. and Dong, Z.Q. (2021), "Dynamic test and numerical simulation on avoiding the weak-story failure mechanism in structures using LSFs", *Steel Compos Struct.*, **40**(2), 175-191. <https://doi.org/10.12989/scs.2021.40.2.175>.
- Zhu, R., Guo, T., Mwangilwa, F. and Han, D. (2021), "Seismic design of self-centering viscous-hysteretic devices used for steel moment-resisting frames", *Eng. Struct.*, **239**, 112369. <https://doi.org/10.1016/j.engstruct.2021.112369>.

## Appendix A Design parameters of frame-shear wall structure

The height of the first floor of the structure is 4.5 meters, the height of the second floor is 4 meters, and the heights of the remaining floors are 3.5 meters. The spans are all 7.5 meters. The height of the low-strength concrete area is 0.5 meters. The equivalent uniformly distributed dead load and live load on the frame beam are 20 kN/m and 10 kN/m respectively. Columns are made of C45 grade concrete, beams are made of C40 grade concrete. The upper wall of the gradient mechanism shear wall is made of C45 concrete. The longitudinal bars of beams, columns and walls and buckling-restrained steel bars are all made of HRB400 grade steel bars. Stirrups are all made of HPB300 grade steel bars. The seismic fortification parameters are as follows: seismic fortification intensity is 8 degrees, the design basic seismic acceleration is 0.20 g, the design earthquake group is the first group, the site category is Class II, the site characteristic period is 0.35 seconds, the seismic fortification category is Class B, and the seismic grade of the structure is first grade.

## Appendix B Component additional damping ratio and equivalent damping ratio of the overall structure

The additional damping ratios of low-strength concrete components and buckling-restrained steel bar groups and the equivalent damping ratio of the overall structure in the stages of good service, damage control and preventing collapse are shown in Table B.1. Frame beams and the bottom column bases are in an elastic state in both the good service and damage control stages, so the additional damping ratios are both  $\zeta_a=0$ . The additional damping ratios of frame beams and the bottom column bases in the stage of preventing collapse are shown in Tables B.2 and B.3 respectively. The expected non-damaged components of the structure never enter the damaged state, so their additional damping ratios are always  $\zeta_a=0$ .

Table B.1 Additional damping ratio of components and equivalent damping ratio of whole structure

Functions	Serviceability	Damage Control		Collapse Prevention
Seismic Fortification	Minor	Medium-minor	Moderate	Major
$\zeta_{eq}$	0.05	0.05	0.0512	0.103
$\zeta_a$	0	0	0.25	0.50
$\zeta_a$	0	-	-	-

Note: The symbol “-” indicates that the low-strength concrete parts are out of work

Table B.2 Additional damping ratio of frame beam during collapse prevention stage

Floors	AB Span	BC Span	CD Span	DE Span
8	0	0	0	0
7	0.14	0.13	0.16	0.22
6	0.29	0.27	0.26	0.27
5	0.32	0.31	0.30	0.30
4	0.21	0.17	0.18	0.22
3	0.23	0.21	0.22	0.25
2	0.27	0.25	0.24	0.26
1	0.30	0.24	0.23	0.29

Table B.3 Additional damping ratio of bottom column foot during preventing collapse stage

Column Feet	A	B	C	D	E
$\zeta_a$	0.33	0.39	0.41	0.4	0.35

## Appendix C

Table C.1 Examples of bearing capacity reference indicators for structural components to meet the requirements of seismic performance

Performance Requirements	Minor Earthquakes	Moderate Earthquakes	Major Earthquakes
Performance 1	Intact, designed according to conventional methods.	Intact, and the bearing capacity shall be rechecked with the design value of seismic effects adjusted according to the seismic fortification level.	Basically intact, and the bearing capacity shall be rechecked with the design value of seismic effects without adjusting according to the seismic fortification level.
Performance 2	Intact, designed according to conventional methods.	Basically intact, and the bearing capacity shall be rechecked with the design value of seismic effects without adjusting according to the seismic fortification level.	Slight to moderate damage, and the bearing capacity shall be rechecked with the ultimate value.
Performance 3	Intact, designed according to conventional methods.	Slightly damaged, and the bearing capacity shall be rechecked with the standard value.	Moderate damage, and the bearing capacity can remain stable after reaching the ultimate value, with a reduction of less than 5%.
Performance 4	Intact, designed according to conventional methods.	Slight to moderate damage, and the bearing capacity shall be rechecked with the ultimate value.	Not severely damaged, and the bearing capacity can basically remain stable after reaching the ultimate value, with a reduction of less than 10%.

Table C.2 Examples of inter - story drift reference indicators for structural components to meet the requirements of seismic performance

Performance Requirements	Minor Earthquakes	Moderate Earthquakes	Major Earthquakes
Performance 1	Intact, with deformation far less than the elastic displacement limit.	Intact, with deformation less than the elastic displacement limit.	Basically intact, with deformation slightly larger than the elastic displacement limit.
Performance 2	Intact, with deformation far less than the elastic displacement limit.	Basically intact, with deformation slightly larger than the elastic displacement limit.	With slight plastic deformation, and the deformation is less than twice the elastic displacement limit.
Performance 3	Intact, with deformation significantly less than the elastic displacement limit.	Slightly damaged, with deformation less than twice the elastic displacement limit.	With obvious plastic deformation, and the deformation is approximately four times the elastic displacement limit.
Performance 4	Intact, with deformation less than the elastic displacement limit.	Slight to moderate damage, with deformation less than three times the elastic displacement limit.	Not severely damaged, with deformation not greater than 0.9 times the plastic deformation limit.

Note: In the calculation of deformation under the moderate and major earthquakes, the second-order effect of gravity should be considered, and the overall bending deformation can be deducted